AIMS Geosciences

AIMS Geosciences, 9(4): 769–782.
DOI: 10.3934/geosci.2023041
Received: 11 October 2023
Revised: 16 November 2023
Accepted: 26 November 2023
Published: 04 December 2023

http://www.aimspress.com/journal/geosciences

Research article

A geophysical insight of the lithostratigraphic subsurface of Rodafnidia area (Lesbos Isl., Greece)

John D Alexopoulos[1], Nikolaos Voulgaris[1], Spyridon Dilalos[1,*], Georgia Mitsika[1], Ioannis-Konstantinos Giannopoulos[1], Vassileios Gkosios[1] and Nena Galanidou[2]

[1] Department of Geology and Geoenvironment, National and Kapodistrian University of Athens, Panepistimioupoli Zografou, 15784, Athens, Greece
[2] Department of History and Archaeology, University of Crete, Rethymno, 74100, Greece

* **Correspondence:** Email: sdilalos@geol.uoa.gr; Tel: +302107274426.

Abstract: The study area of Rodafnidia on the island of Lesbos (Greece) is considered of archaeological interest, as Paleolithic stone tools have been recovered through excavation and collected from the ground surface in recent years. Geologically, the area is mostly covered by Quaternary post-alpine deposits and volcanic rocks. This paper presents the application of a local geophysical survey to determine the volume of the upper Quaternary deposits in which the Paleolithic artefacts can be found and the identification of their ignimbrite substrates. For this reason, the geoelectrical method was selected as the most appropriate for determining the lithostratigraphic subsurface layers. More specifically, a grid of twenty-one (21) Vertical Electrical Soundings (VES) along with an Electrical Resistivity Tomography (ERT) was carried out. The interpretation of the results of these surveys, in conjunction with the results of older excavation trenches, revealed that the Quaternary deposits have been investigated at depths ranging from 0.5 up to 28.5 meters. Furthermore, the lithological boundary of these post-alpine deposits and their underlying pyroclastic ignimbrite flow (with resistivity 24.0–58.0 Ohm.m) seem to dip to the north. The volume of the Quaternary layer is proposed as the maximum depth for archaeological investigation with high chances to recover more Paleolithic material.

Keywords: ignimbrite; Vertical Electrical Sounding; Electrical Resistivity Tomography; geoelectrical method; paleolithic; archaeology

1. Introduction

Rodafnidia area is close to a hilly area at Lisvori village, on the south part of the island of Lesbos (Greece), at the north-east Aegean Sea (Figure 1). It is an area of archaeological interest where Lower Paleolithic remains have been recently found at the surface, inside the Quaternary post-alpine formations [1]. The landscape of the area has been determined by the local volcanism and tectonism and for that reason the findings are expected to be found only in the upper alluvial deposits that are overlying the volcanic formation of ignimbrite.

In the context of the archaeological survey conducted by the University of Crete, several small pits and 34 trenches have been excavated (Figures 1 and 2) and are presented in detail in older publications [1,2]. Their depth of investigation in some cases have reached 6.0 meters, exposing stratigraphic sequences at shallow depths.

According to the archaeological finds and the high potential for more to be recovered from Rodafnidia and its wider vicinity, it is crucial to determine the geological subsurface of the area with the contribution of geophysical methods in order to plan the future steps of the archaeological investigation. More specifically, the scope of the geophysical survey is to reveal the bottom of the Quaternary post-alpine formations, which is practically their boundary with their underlying volcanic rock of ignimbrite. This is expected to provide valuable information to archaeologists by indicating the maximum depth of potentially find-bearing deposits across the area of interest.

The selected geoelectrical method for investigating the area has been successfully applied in the past for geological and lithostratigraphic investigations [3–9]. This method has also been carried out successfully to similar geological environments, with the occurrence of ignimbrites [10–21].

Based on similar archaeological investigations with the contribution of geophysical measurements [22,23], we have to take into consideration the disturbances that may occur during the data acquisition. There are several factors that may affect the geophysical data based on [24], such as the artificial noise, which can be industrial (e.g., due to transport systems), instrumental or due to difficulties in the electrode grounding (for which special care had been given during the field measurements).

On the other hand, we have natural disturbances, including meteorological, soil and vegetable factors, categorized as nonstationary noise. Beyond these, there is also the "stationary" noise category, including the rough terrain relief affecting the accessibility of the area but also the complexity of the underground structure of geoarchaeological environments. In our case, this noise disturbance is minimized, given the fact that we don't have structural archaeological settlements.

2. Geology of the area

The geological structure of Lesbos Island is composed mostly of Middle Miocene volcanic rocks, volcanic deposits, such as ignimbrites and tuffs but also Quaternary post-alpine deposits, which have been studied thoroughly by other researchers [1,25–31].

Based on the geological mapping of IGME [25], the upper formation of the area is practically the Alluvial plains (Q.al), which consist of clays (gray & red), sands, gravels, coastal sands and fluvial deposits but can also contain siliceous clastic elements [1]. The extent of the alluvial deposits has been updated (Figure 1) based on the macroscopic geological observations of the research team. The formation of Marls and tuffites (Pl.m) is located mainly at the north-eastern part of the greater

area, with intercalated white limestones that are partly silicified, observed with a maximum thickness of 120 meters.

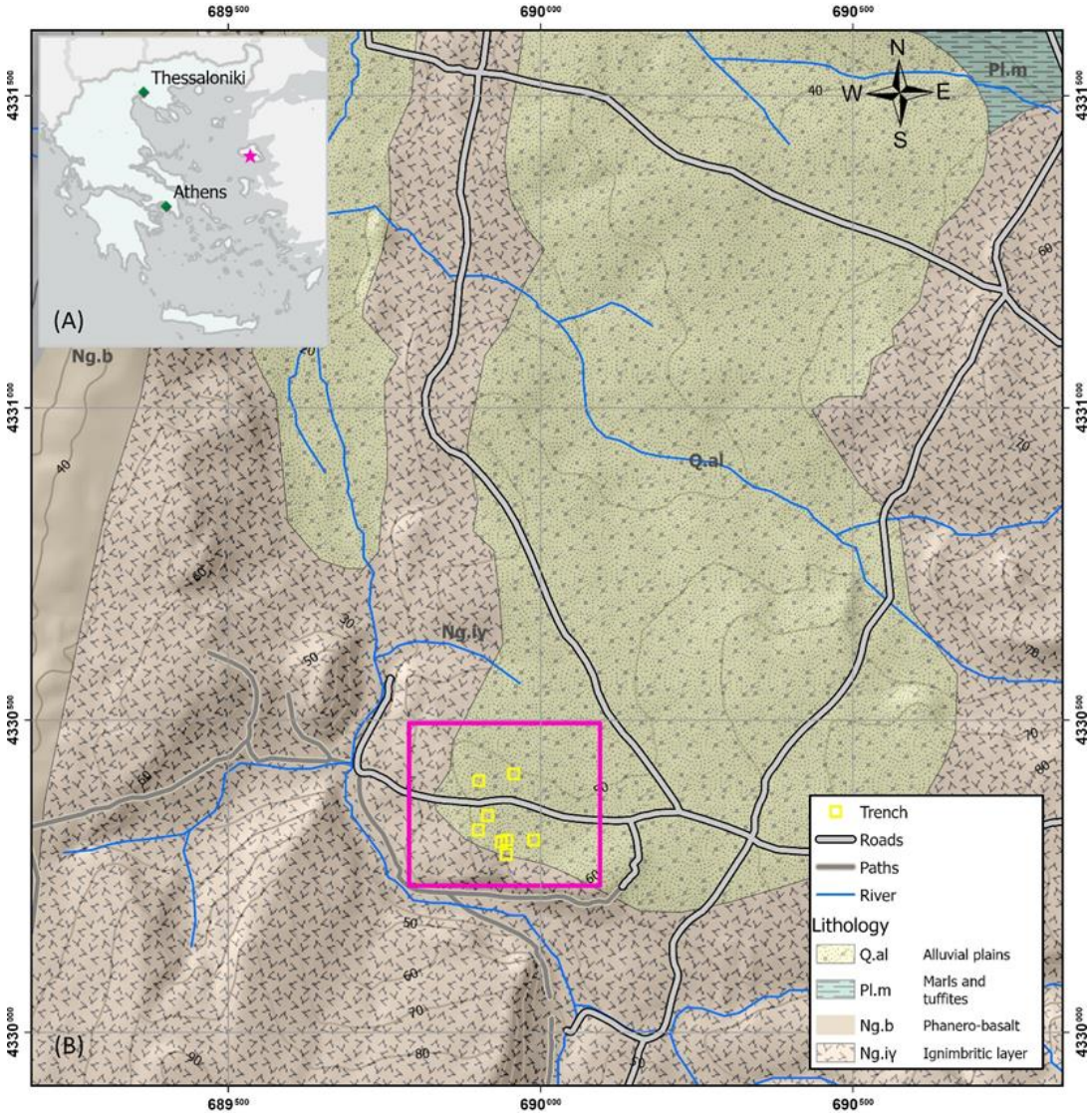

Figure 1. a) Index map of the area; b) Modified geological map by IGME [22] of the greater study area. The pink box indicates the study area of Rodafnidia.

The excavated trenches, conducted up to 6.0 meters depth, revealed in greater detail the stratigraphy of the surficial alluvial plains (Q.al). These mostly consist of clays, gravels and sands, while a formation of conglomerates can be found underlying them [1,2].

Beyond the two prementioned, post-alpine formations, there are two extrusive volcanic rock formations (Figure 1). The Phanero-basalt (Ng.b) formation, which is partly basaltic agglomerates, found underlying the pyroclastic layer (Ng.pc) and in the Ignimbritic layer (Ng.ιγ) made of rhyolitic to rhyodacitic welded tuff that is overlain by the Pliocene freshwater sediments, observed with a thickness up to 120 meters. The ignimbrite formation is considered to be the substrate of the area based on the authors of [2], who also mention that two main sub-areas have been revealed from the stratigraphic results of the excavation trenches in the greater area. Between them, the formation of ignimbrite is close to the surface or even revealed as an outcrop.

According to the authors of [32], the greater area is controlled by two major faults, the "Agia Paraskeyi" across the Gulf of Kalloni (direction NE-SW) and the "Vrisa" one (direction NW-SE). They are not indicated in Figure 2 since they are out of its boundaries. Their geological history indicates that the greater area has been land at least from Middle Pleistocene.

3. Geophysical survey

The geoelectrical method was mainly selected in order to determine the boundaries of the ignimbrite formation, known for its successful applications in the past [10–21]. Two techniques were applied, the Vertical Electrical Soundings (VES) for the vertical investigation of the resistivity distribution and the high-resolution technique of Electrical Resistivity Tomography (ERT) for the 2D subsurface investigation of the resistivity distribution.

3.1. Field data acquisition

Twenty-one (21) Vertical Electrical Soundings (VES) with Schlumberger array were performed at the area of Rodafnidia, as planned on a local grid (Figure 2). The selected electrode spacings (AB) of VES measurements were 2.0, 3.0, 4.3, 6.3, 9.0, 14.0, 20.0, 30.0, 43.0, 63.0, 93.0, 136, 200 and 300 meters, leading to a maximum investigation depth of almost 60.0 meters. In the context of determining the resistivity of the ignimbrite at the investigated area, one (1) "in-situ" VES was carried out on a local outcrop of ignimbrite (Figure 2). An ABEM Terrameter unit has been used for the acquisition of the VES measurements.

Apart from the VES measurements, a 160-m Electrical Resistivity Tomography (ERT) was conducted, based on the first processing results of the VES. It was acquired in a N-S direction, along the middle set of soundings 08–13 (Figure 2). Therefore, a dataset of 997 measurement points of apparent resistivity was collected using the Wenner array with an electrode spacing of 1.0 meter with the roll-along technique. The ERT measurements were collected using the ABEM Terrameter Unit, supported by the Lund Imaging System. Additional topographic leveling measurements were collected in order to embed them to the inversion procedure of the ERT data due to a minor relief of the area. The geodetic system used for these coordinates was the EGSA'87 (Datum GGRS'80).

3.2. Processing

As a first approach, a pseudo-3D set of horizontal pseudo-depth (AB/2) slices for the distribution of the apparent resistivity [33,34] were produced, for current electrode spacing AB equal to 3.0, 4.3, 6.3, 9.0, 14.0, 20.0, 30.0, 43.0, 63.0 and 93.0 meters (Figure 3). Regarding the smaller spacings, up to AB = 4.3 meters (estimated investigation depth equal to 1 meter), relatively more resistant geoelectrical formations have been investigated (>25.0 Ohm.m). For AB spacing 6.3 to 14.0 meters (estimated investigation depths 1.5–3.0 meters), more conductive formations have been revealed (<25.0 Ohm.m), with the exception of some areas at the SSE part.

The VES data were processed by applying the automatic method of Zohdy and Bisdorf [35], composing a "multilayer" geoelectrical model. Beyond this, the commercial software package IX1D of Interpex, was used in order to determine the corresponding "layered" geoelectrical model of each sounding. The processing results of the "multilayer" geoelectrical models allow the creation of the

three (3), almost parallel (Figure 2), resistivity distribution sections (Figure 4), with S-N direction.

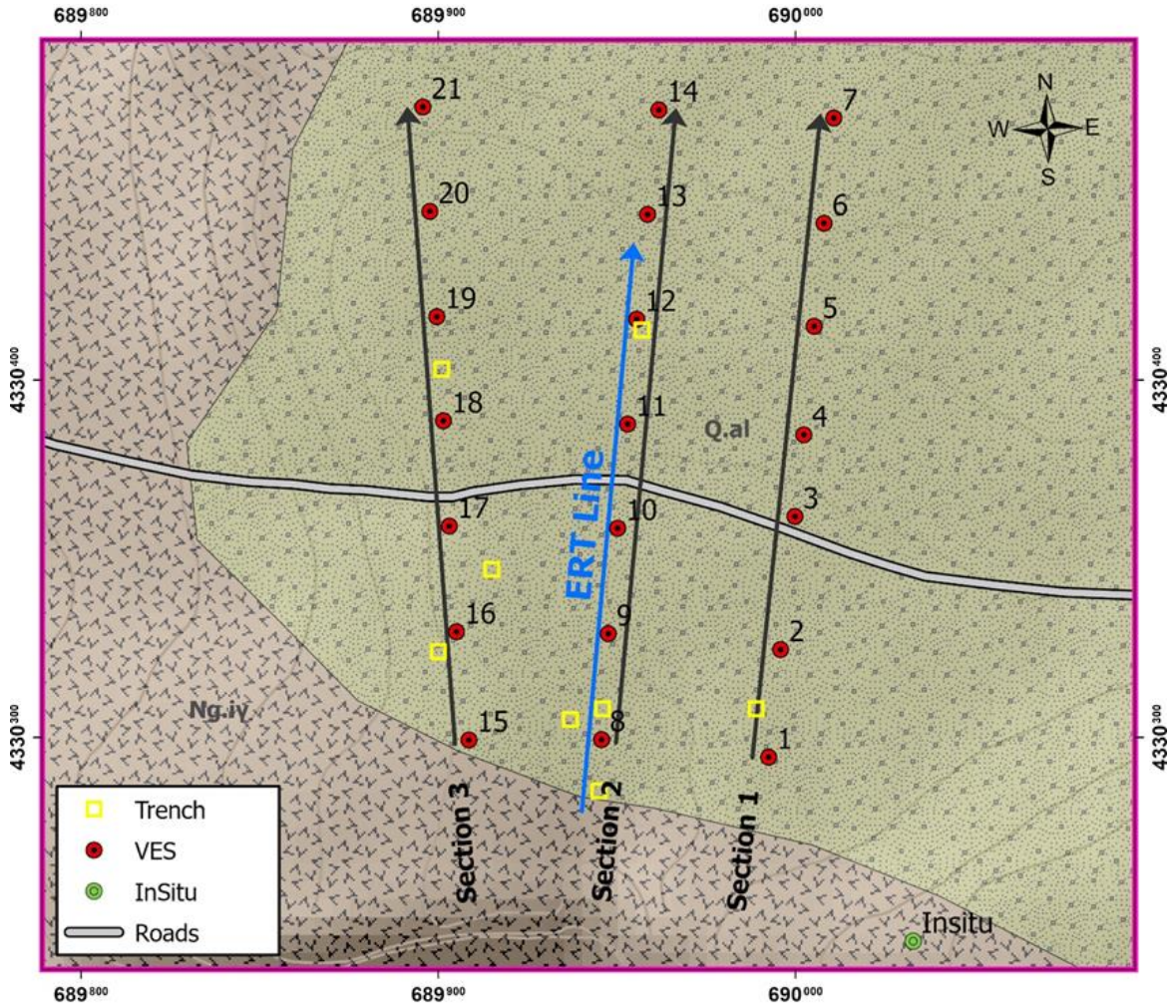

Figure 2. The locations of all the acquired geophysical measurements in the study area.

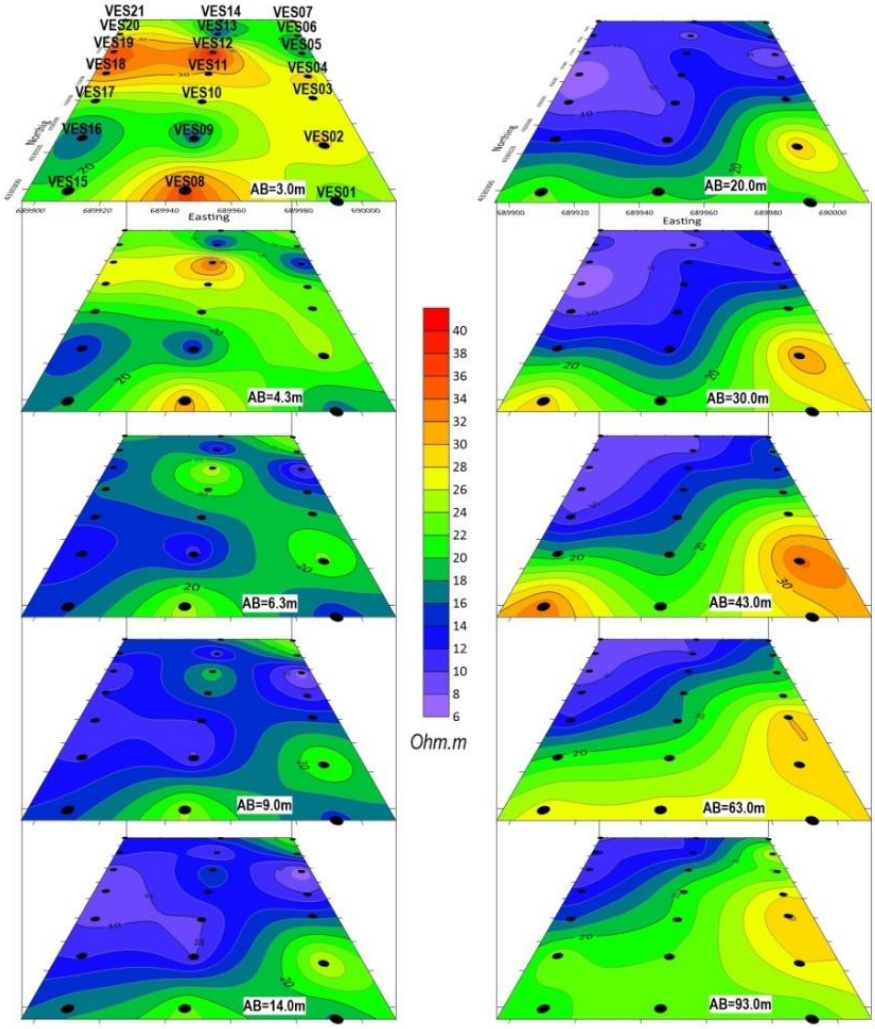

Figure 3. Horizontal pseudo-depth (AB/2) slices for the distribution of the apparent resistivity in the study area.

Along all three resistivity sections (Figure 4), the following common characteristics are observed:

- A very shallow geoelectrical formation, with resistivity values ranging from 19.0 to 44.0 Ohm.m.
- Beyond that, a more conductive geoelectrical layer is also observed along all sections, with resistivity values 6.0–15.0 Ohm.m. It dipps to the North, at depths ranging from 0.5 to even 30.0 meters. At section 3, its extension is smaller than in the other two sections.
- A more resistant underlying geoelectrical layer was also investigated along all sections, with resistivity values from 20.0 up to 57.0 Ohm.m, at depths from 14.5 (section 1) up to 76.0 meters (section 3).
- The geoelectrical basement of all sections is characterized by resistivity values ranging from 5.0 to 19.0 Ohm.m. The only areas that were not revealed are below VES 14 (section 2) and VES 19–21 (section 3).

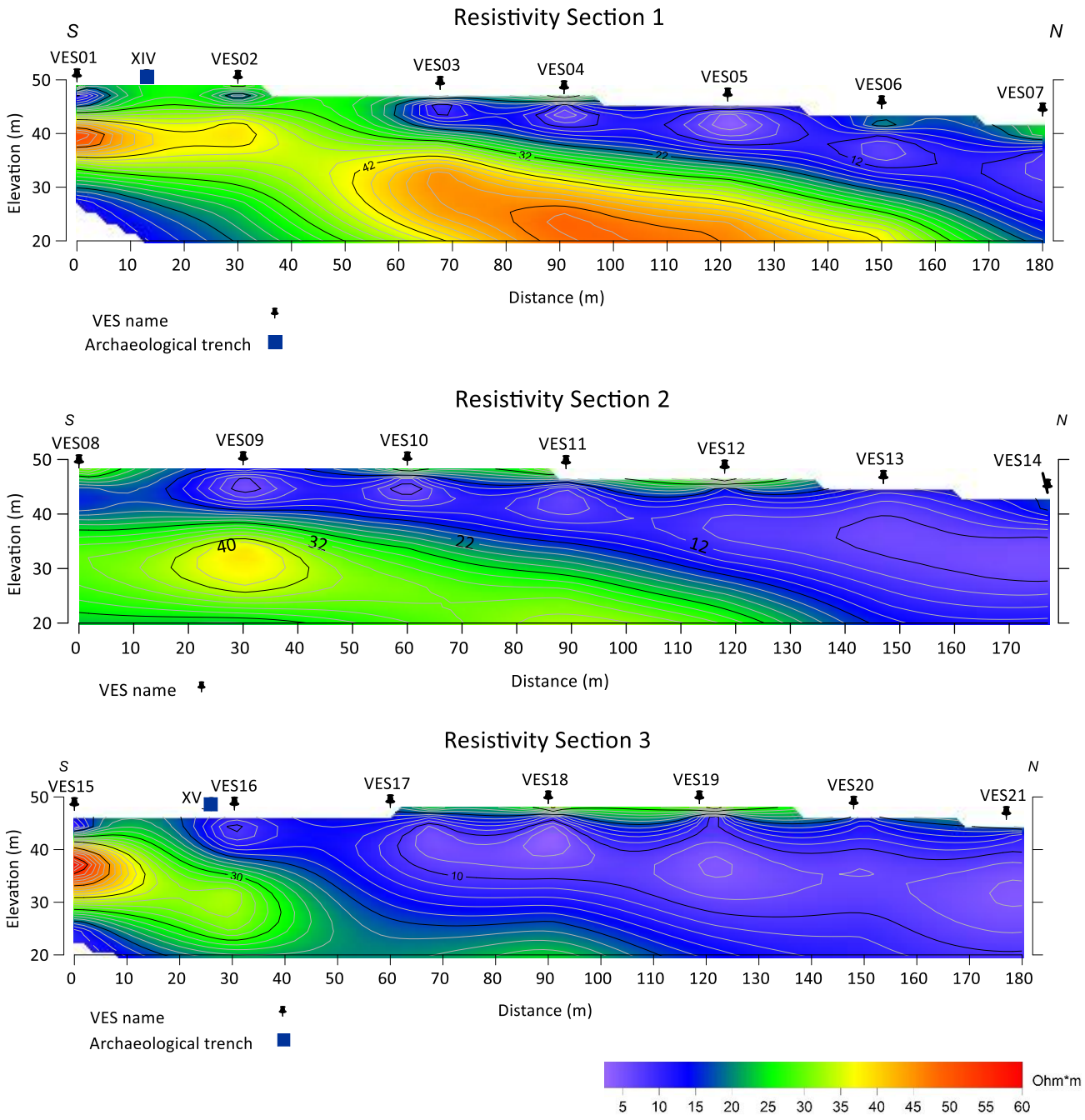

Figure 4. Resistivity sections.

The ERT data were processed with the RES2DINV software (GeoTomo) and are illustrated in Figure 5. The acquired topographic measurements of each section were been taken into consideration during the inversion process due to the relief of the study area. The processing software iteratively calculates a resistivity model, trying to minimize the difference between the observed apparent resistivity values and those calculated from the model. The inversion process is continuously repeated until the minimum possible misfit is reached. The inversion results illustrated in Figure 5 were obtained after 6 iterations, with an RMS error of 4,38%.

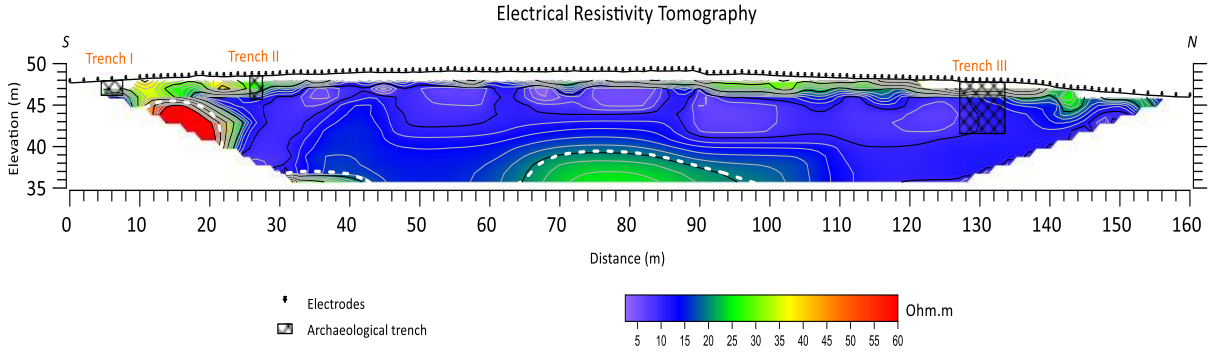

Figure 5. Electrical Resistivity Tomography inversion results. The locations of the archaeological trenches are also illustrated.

In general, across the ERT of Figure 5, relatively small resistivity values (2.0–20.0 Ohm.m) are observed. In the southern part of the section, at small depths, a resistant formation (40.0–62.0 Ohm.m) was adumbrated, but it practically disappears at the distance of 25.0 meters across the section. At the central part of the section and at an approximate depth of 8.0 meters, a less resistant formation (20.0–33.0 Ohm.m) was investigated.

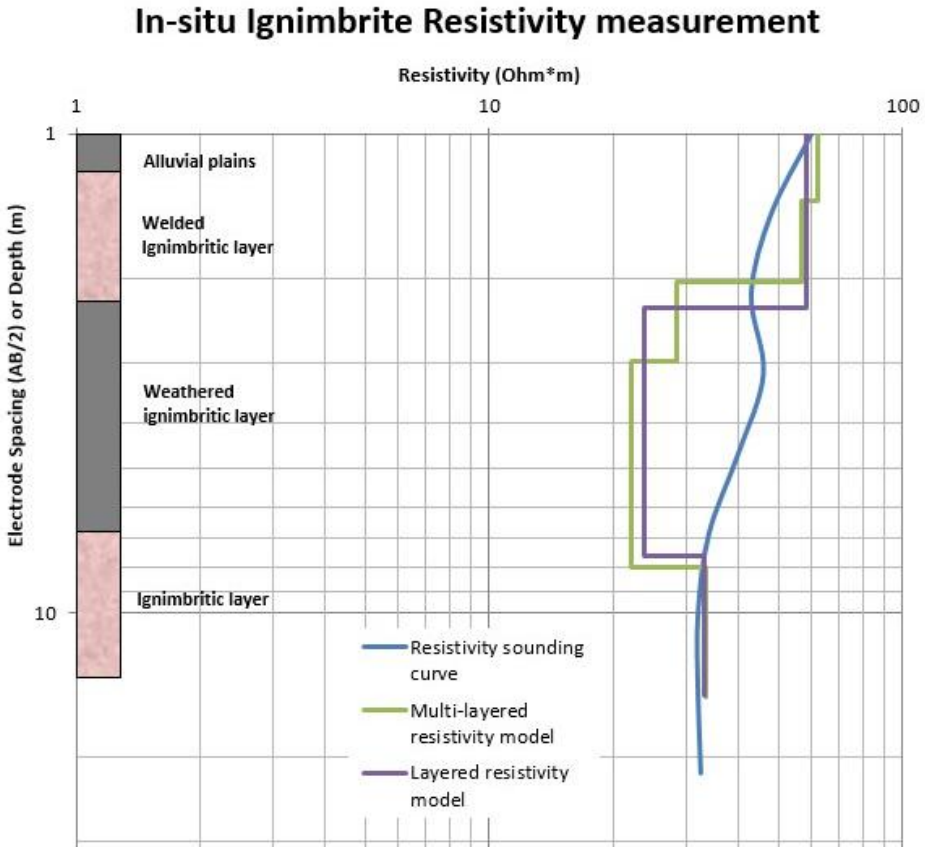

Figure 6. The results of the in-situ VES measurements on the ignimbrite formation. Its location is illustrated on Figure 2.

4. Discussion—Interpretation

Based on all the geophysical results—including the ones of the in-situ sounding on the ignimbrite (Figure 6)—along with the geological and strata data at the excavated trenches of the study area [1,2], the Geological-Geophysical Sections of Figure 7 were produced, revealing the subsurface geological-lithostratigraphic structure of the investigated area.

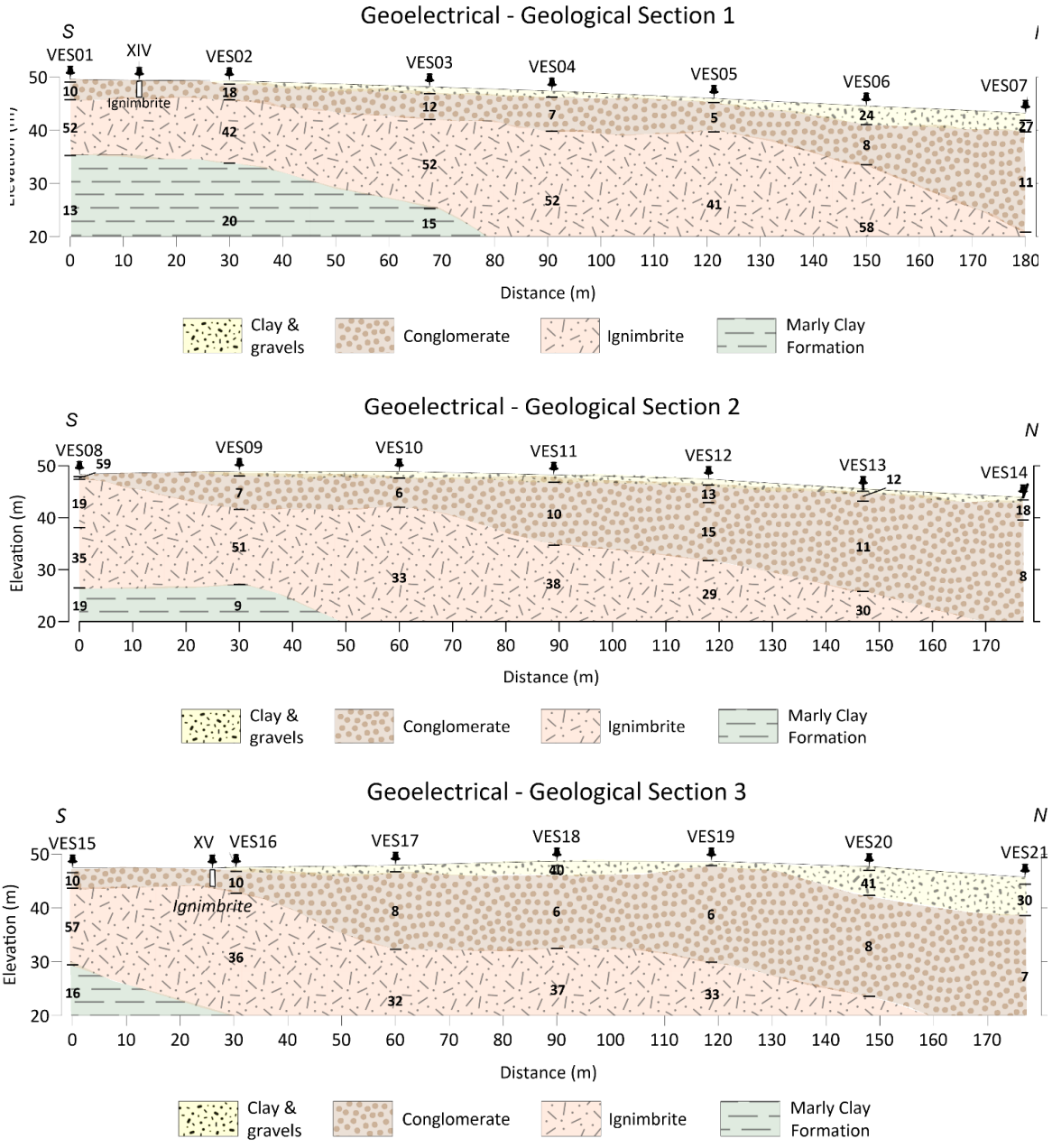

Figure 7. Geoelectrical-Geological Sections.

More specifically, in Figure 7 we can observe the following common interpreted lithostratigraphic units:

- An upper relatively conductive layer (20.0–40.0 Ohm.m) which seems to correspond to the formation of clays and gravels, with thickness from 0.5 up to 3.5 meters.

- An underlying conglomerate formation (*Q.al*) of lower resistivity values (5.0–18.0 Ohm.m), probably due to its water saturation. Its thickness ranges from 0.5 to 28.5 meters and dips to the North.
- Below the interpreted conglomerates, the most resistant formation (24.0–58.0 Ohm.m) was related to the Miocene pyroclastic flows of the ignimbrite. It also dips to the north and has an average thickness of almost 10.5 meters.
- The deeper lithostratigraphic unit, with resistivity values of 6.0–20.0 Ohm.m, has been interpreted as the marly clay formation. It is considered as the geological basement of the study area and the boundary over which the pyroclastic was flown on.

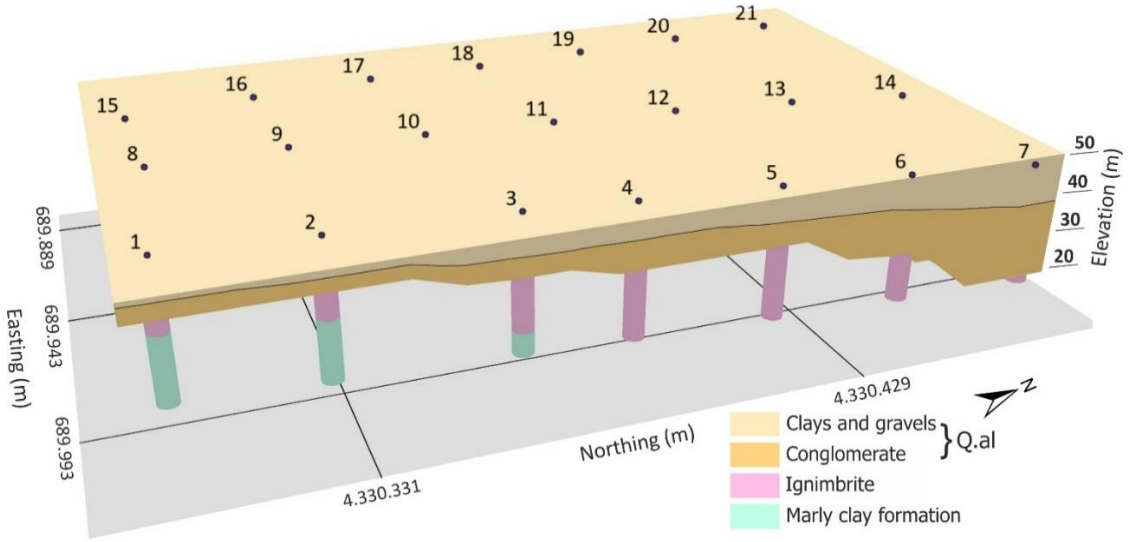

Figure 8. 3D representation of the lithological boundaries determined by the geophysical interpretation.

In Figures 7 and 8, the pyroclastic flows follow the relatively smooth paleo-relief of the marly-clay lithostratigraphic unit, dipping to the north. In Figure 8, a 3D representation of the lithological boundaries determined by the geophysical interpretation is presented and constructed with *Rockworks* software. The upper, yellowish, layers of Figure 8 represent the volume of the Quaternary deposits, which corresponds to the area of probable future archaeological excavations. The geological interpretation of the VES soundings below these two post-alpine lithostratigraphic units is also illustrated as boreholes in order to present the geological substrate of the area, comprised of the ignimbrite & marls [2]. The bottom surface of the yellowish volume corresponds to the boundary between the Quaternary deposits and the pyroclastic flow of the ignimbrite.

Based on these interpretation sections (Figure 7), the corresponding resistivity range values of each lithostratigraphic units have been summarized in Table 1. Similar resistivity values for ignimbrites have also been revealed in the past by other researchers [13,16,18,19,21].

The results of the geophysical survey can provide the new guidelines determining the depths of interest for the future archaeological excavations. Based on all three sections in Figure 7, it is clear that there is a general dip of the ignimbrite boundary to the north, which means that the expected depths of excavation will increase from south to north. Archaeologists could probably prioritize the excavation in shallower sections, located south of the area, in order to retrieve sooner any possible finds. Beyond that, the cost and workload of the excavations will be less.

Table 1. Resistivity values of the geological formations.

Geological formation	Resistivity (Ohm.m)
Clays & gravels	24.0–41.0
Conglomerate	5.0–18.0
Ignimbrite (*Ng.ιγ*)	24.0–58.0
Marly Clay formation	6.0–20.0

The comparison of the two different techniques that have been applied (VES and ERT) in the area reveals a good congruency in general, providing quite similar geoelectrical distributions. The ERT has investigated smaller depths than the VES, but in greater detail. Regarding their common depth of investigation, which is almost 15 meters, we do not observe great differences apart from the better detail of the ERT. At this point, wewould like to remind that the VES soundings were applied at first for deeper investigation, without knowing the exact depths of the ignimbrite. After the results and depth determination, the ERT was carried out as an additional investigation detailed method for the upper layers.

5. Conclusions

The geophysical survey conducted in the area of Rodafnidia has adequately revealed the subsurface lithostratigraphic structure. This subsurface information can be taken advantage of by the archaeologists of the area in order to plan in a better way their forthcoming excavations, based on the presence/absence and thickness of potentially find-bearing geological units. The adumbration of the upper boundary of the ignimbrite substrate geological formation can set the maximum depth of interest for archaeological investigation. This is due to the fact that the lithic artefacts have been found only in the overlying Quaternary post-alpine lithostratigraphic units, consisting of clays, gravels, sands and conglomerates. The interpreted geophysical results revealed that the maximum excavation depth ranges from 0.5 up to 28.5 meters at the northern part of Rodafnidia area.

Acknowledgments

The data acquisition was funded in the context of the research program "*Paleolithic Lesbos*". The authors would like to acknowledge Dr. Iliopoulos G. and Dr. Sakellariou D. for their valuable discussions regarding the geological environment of the area. Additionally, the authors would like to thank Petras A. and Kastoras D. for their contribution to the field measurements.

Use of AI tools declaration

The authors declare that they have not used Artificial Intelligence (AI) tools in the creation of this article.

Conflict of interest

The authors declare no conflicts of interest in this paper.

References

1. Galanidou N, Athanassas C, Cole J, et al. (2016) The acheulian site at rodafnidia, Lisvori, on Lesbos, Greece: 2010–2012, *Paleoanthropology of the Balkans and Anatolia: Human evolution and its context*, Springer, Dordrecht. 119–138. https://doi.org/10.1007/978-94-024-0874-4_8
2. Iliopoulos G, Alexopoulos J, Papadopoulou P, et al. (2022) The Acheulean site of Rodafnidia: geology, stratigraphy and chronology. *Aegean Acheulean at the Eurasian crossroads Hominin settlement in Eurasia and Africa*: 3–5, 25–29, Lesbos, Greece.
3. Tian S, Zhang P, Shang T, et al. (2022) Application of resistivity sounding in Quaternary stratigraphic division in Yixing, Eastern China. *J Geophys Eng* 19: 362–375. https://doi.org/10.1093/jge/gxac025
4. Alexopoulos JD, Dilalos S, Mitsika GS, et al. (2019) The Contribution of Geophysical Survey to Seismic Hazard Mapping at Farsala basin (Greece). *Bull Geol Soc Greece*.
5. Alexopoulos JD, Dilalos S, Voulgaris N, et al. (2023) The Contribution of Near-Surface Geophysics for the Site Characterization of Seismological Stations. *Appl Sci* 13: 4932. https://doi.org/10.3390/app13084932
6. Alexopoulos JD, Dilalos S (2010) Geophysical research for geological structure determination in the region of South Mesogheia (Attica). *Bull Geol Soc Greece* 43: 1898–1906. https://doi.org/10.12681/bgsg.11381
7. Fountoulis I, Vassilakis E, Mavroulis S, et al. (2015) Synergy of tectonic geomorphology, applied geophysics and remote sensing techniques reveals new data for active extensional tectonism in NW Peloponnese (Greece). *Geomorphology* 237: 52–64. https://doi.org/10.1016/j.geomorph.2014.11.016
8. Mitsika GS, Alexopoulos JD, Vassilakis E, et al. (2023) Investigation of the physical-geographical characteristics of river delta with geophysical and satellite data. The case study of Pineios River, Greece. *MethodsX* 10: 102033. https://doi.org/10.1016/j.mex.2023.102033
9. Papadopoulos TD, Alexopoulos JD, Dilalos S (2020) Combined geoelectrical and geoelectromagnetic survey for contributing to local hydrogeological regime—The case study of Delfini basin (Chios isl.—Greece). *Geol Geophys Russ South* 10: 68–80. https://doi.org/10.23671/VNC.2020.1.59066
10. Abdulkadir YA, Eritro TH (2017) 2D resistivity imaging and magnetic survey for characterization of thermal springs: a case study of Gergedi thermal springs in the northwest of Wonji, Main Ethiopian Rift, Ethiopia. *J Afr Earth Sci* 133: 95–103. https://doi.org/10.1016/j.jafrearsci.2017.05.001
11. Bibby HM, Bennie SL, Stagpoole VM, et al. (1994) Resistivity structure of the Waimangu, Waiotapu, Waikite and Reporoa geothermal areas, New Zealand. *Geothermics* 23: 445–471. https://doi.org/10.1016/0375-6505(94)90013-2
12. Bibby HM, Caldwell TG, Risk GF (1998) Electrical resistivity image of the upper crust within the Taupo Volcanic Zone, New Zealand. *J Geophys Res: Solid Earth* 103: 9665–9680. https://doi.org/10.1029/98JB00031
13. Bibby HM, Risk GF, Caldwell TG (2002) Long offset tensor apparent resistivity surveys of the Taupo Volcanic Zone, New Zealand. *J Appl Geophys* 49: 17–32. https://doi.org/10.1016/S0926-9851(01)00096-9

14. Bibby HM, Risk GF, Caldwell TG, et al. (2008) Resistivity structure of western Taupo Volcanic Zone, New Zealand. *N Z J Geol Geophys* 51: 231–244. https://doi.org/10.1080/00288300809509862
15. Fisseha S, Mewa G, Haile T (2021) Refraction seismic complementing electrical method in subsurface characterization for tunneling in soft pyroclastic (a case study). *Heliyon* 7: e07680. https://doi.org/10.1016/j.heliyon.2021.e07680
16. İlkişik OM, Gürer A, Tokgöz T, et al. (1997) Geoelectromagnetic and geothermic investigations in the Ihlara Valley geothermal field. *J Volcanol Geotherm Res* 78: 297–308. https://doi.org/10.1016/S0377-0273(97)00008-5
17. Longo V, Testone V, Oggiano G, et al. (2014) Prospecting for clay minerals within volcanic successions: Application of electrical resistivity tomography to characterise bentonite deposits in northern Sardinia (Italy). *J Appl Geophys* 111: 21–32. https://doi.org/10.1016/j.jappgeo.2014.09.014
18. Markos M, Saka A, Jule LT, et al. (2021) Groundwater potential assessment using vertical electrical sounding and magnetic methods: A case of Adilo Catchment, South Nations, Nationalities and Peoples Regional Government, Ethiopia. *Concepts Magn Reson* 2021: 1–11. https://doi.org/10.1155/2021/5424865
19. Risk GF, Bibby HM, Caldwell TG (1993) DC resistivity mapping with the multiple-source bipole-dipole array in the Central Volcanic Region, New Zealand. *J Geomagn Geoelectr* 45: 897–916. https://doi.org/10.5636/jgg.45.897
20. Risk GF, Caldwell TG, Bibby HM (1994) Deep resistivity surveys in the waiotapu-Waikite-Reporoa region, New Zealand. *Geothermics* 23: 423–443. https://doi.org/10.1016/0375-6505(94)90012-4
21. Risk GF, Bibby HM, Caldwell TG (1999) Resistivity structure of the central Taupo volcanic zone, New Zealand. *J Volcanol Geotherm Res* 90: 163–181. https://doi.org/10.1016/S0377-0273(99)00026-8
22. Eppelbaum LV, Itkis SE, Khesin BE (2006) Detailed magnetic survey unmasks Prehistoric archaeological sites in Israel. *19th EEGS Symposium on the Application of Geophysics to Engineering and Environmental Problems*. European Association of Geoscientists & Engineers. https://doi.org/10.3997/2214-4609-pdb.181.138
23. Eppelbaum LV, Khesin BE (2001) Disturbing factors in geophysical investigations at archaeological sites and ways of their elimination. *Transactions of the IV Conference on Archaeological Prospection*, *Vienna, Austria,* 99–101.
24. Eppelbaum LV, Khesin BE, Itkis SE (2010). Archaeological geophysics in arid environments: Examples from Israel. *J Arid Environ* 74: 849–860. https://doi.org/10.1016/j.jaridenv.2009.04.018
25. Hecht J (1974) Geological map of Greece, Sheet Polichnitos (Lesbos Island), Scale 1:50.000. National Institute of Geological and Mining Research (IGME). Athens, Greece.
26. Lamera S, Seymour KS, Vamvoukakis C, et al. (2001) The Polychnitos ignimbrite of Lesvos island. *Bull Geol Soc Greece* 34: 917–921. https://doi.org/10.12681/bgsg.17118
27. Lamera S (2004) The Polichnitos ignimbrite of Lesvos island. Ph.D. Thesis University of Patras (in Greek): 272. http://hdl.handle.net/10442/hedi/26632
28. Pe-Piper G (1978) The Cenozoic volcanic rocks of Lesbos. Ph.D. Thesis, University of Patras. (in Greek).

29. Pe-Piper G, Piper DJW (1993) Revised stratigraphy of the Miocene volcanic rocks of Lesbos, Greece. *Neues Jahrb Geol P-M* 2: 97–110. https://doi.org/10.1127/njgpm/1993/1993/97
30. Pe-Piper G, Piper DJW (2002) The igneous rocks of Greece. The Anatomy of an Orogen. Gebrüder Borntraeger-Berlin, Stuttgart. *G. Catsadorakis: Determinants of raptor abundance,* 573.
31. Thomaidou EL (2009) Geological structure of Lesbos Island. Ph.D. Thesis Aristotelian University of Thessaloniki: 199. (in Greek). http://hdl.handle.net/10442/hedi/19792
32. Sotiropoulou S, Kalaitzis M, Sakellariou D, et al. (2022) Plio-Quaternary palaeogeographic evolution of central south Lesbos: implications for Palaeolithic Archaeology. *Aegean Acheulean at the Eurasian crossroads Hominin settlement in Eurasia and Africa:* 14–15: 25–29. Lesbos, Greece.
33. Alexopoulos J, Dilalos S, Mitsika GS, et al. (2019) A geophysical approach to the phenomenon of ground fissures at the East Thessaly basin (Greece). *25th European Meeting of Environmental and Engineering Geophysics*, 2019: 1–5.
34. Oudeika MS, Taşdelen S, Güngör M, et al. (2021) Integrated vertical electrical sounding and hydrogeological approach for detailed groundwater pathways investigation: Gökpınar Dam Lake, Denizli, Turkey. *J Afr Earth Sci* 182: 104273. https://doi.org/10.1016/j.jafrearsci.2021.104273
35. Zohdy AA (1989) A new method for the automatic interpretation of Schlumberger and Wenner sounding curves. *Geophysics* 54: 245–253. https://doi.org/10.1190/1.1442648

AIMS Press